JOINT EUROPEAN TORUS

JET–P(92)86

J. O'Rourke, C. Gowers, G.J. Kramer, P.D. Morgan, R. Simonini,
A.C.C. Sips and JET Team

Measurements of the Electron Source Distribution and Particle Transport Coefficients in JET

Measurements of the Electron Source Distribution and Particle Transport Coefficients in JET

J. O'Rourke, C. Gowers, G.J. Kramer[1], P.D. Morgan, R. Simonini,
A.C.C. Sips and JET Team*

JET-Joint Undertaking, Culham Science Centre, OX14 3DB, Abingdon, UK

[1]FOM-Rijnhuizen, Nieuwegein, The Netherlands
** See Annex*

Preprint of Paper to be submitted for publication in
Plasma Physics and Controlled Fusion

ABSTRACT.

Reflectometer measurements of electron density perturbations produced by modulation of the gas feed are used to measure the electron source distribution and benchmark Monte-Carlo neutral transport calculations. An analysis of the temporal evolution of the electron flux calculated using the measured source yields the diffusion coefficient, D_e, and the pinch velocity, V_p. The radial profiles and parametric dependencies of these particle transport coefficients are studied in ohmic and L-mode regimes.

1. INTRODUCTION

Cross field particle transport is an important element of magnetic confinement fusion research. Techniques for fuelling a tokamak, for controlling impurity concentrations, and for removal of the 'fusion ash' will depend critically on the nature of particle transport. Tokamaks are also subject to an operational density limit beyond which a discharge disrupts /1/ or exhibits "MARFE" behaviour /2/, making control of the particle inventory and the density profile important. Finally, theories of anomalous transport make predictions about the relation between particle and thermal transport /3/. Hence the study of particle transport also affords a basis for excluding some contending theories of thermal transport.

An accurate determination of the electron source distribution is an essential prerequisite for the study of particle transport. The electron source profile arises from a number of atomic processes: (1) the ionization of hydrogenic neutrals, (2) ionisation of impurities and (3) recombination of both hydrogenic and impurity ions. The contribution from neutrals is normally infered using neutral transport codes /4,5/ and requires knowledge of plasma parameters and atomic cross-sections. The contribution from impurity ionization requires knowledge of charged-particle transport. Because of the large number of required parameters calculations of the electron source are subject to considerable errors.

Experimental verification of these calculations is also unsatisfactory, as it relies on charge-exchange measurements of the neutral particle distribution /6/, which are not directly related to the electron source. or spectroscopic data, with uncertainties arising from the interpretation of line intensities and the Abel inversion of chordal data /7,8/. The short scale length of the electron source makes the Abel inversion of quantities related to it particularly difficult.

In this paper we report the first direct determination of the electron source distribution in JET from harmonic perturbations of the electron density produced by modulation of the gas feed. This technique uses localised measurements which can be directly related to the electron source distribution. We then present an analysis of electron particle transport in JET which is consistent with this experimentally determined source.

In section 2 we discuss the analysis of the gas modulation experiments from which the electron source distribution (and the electron diffusion coefficient) are obtained. In section 3 the modulation data are presented. The measured source is found to corroborate the results of neutral transport code calculations. Integration of the particle balance equation using this source yields the electron flux. In section 4 an analysis of the temporal evolution of the electron flux, in terms of a transport model which consists of diffusive and non-diffusive terms, is discussed. We find, in agreement with previous analyses, that both the diffusion coefficient and the pinch velocity increase with radius and are strongly anomalous at radii greater than $r/a \sim 0.4$. In section 5 this analysis is extended to a range of JET discharges to study the parametric dependences of the transport coefficients. The diffusion coefficient increases with electron temperature and decreases with poloidal magnetic field. The pinch velocity is found to be proportional to the diffusion coefficient. In section 6 we summarize our results and draw conclusions.

2. ANALYSIS OF GAS MODULATION EXPERIMENTS

In the experiments reported here, modulations of the electron density are produced by modulating the gas feed at 1 to 4 Hz. The modulations are measured by a 12-channel microwave reflectometer /9/, which measures displacements of the critical density layer corresponding to each reflectometer frequency with a sensitivity of about 0.4 mm. Fourier analysis of the data increases the sensitivity and yields the phase and amplitude of the critical layer modulations. The amplitude of the local density modulations is related to the amplitude of the critical layer modulations via the density gradient:

$$\tilde{n}_e = \tilde{R}_{crit} \cdot \frac{\partial n_e(R_{crit})}{\partial R} \qquad [1]$$

Because of this dependence, the amplitude of the density modulations is subject to larger error than their phase. The density gradient is measured by the reflectometer itself, and also by a 6 channel far-infrared interferometer /10/ and a LIDAR Thomson scattering instrument /11/. The density modulations are accompanied by modulations of the electron temperature. These are measured with a 12-channel grating polychromator /12/ and used to provide a consistency check on the amplitude of the density modulations.

The Green's function for the linearized particle balance equation with constant diffusion coefficient is given by

$$\frac{\partial \tilde{n}_e}{\partial t} = D_e \nabla^2 \tilde{n}_e + \frac{\delta(r - r_0)}{4\pi^2 r R} e^{i\omega t}. \qquad [2]$$

The solution is /13/:

$$\tilde{n}_e^{\delta}(r,t, r_0, \omega, D_e) \qquad [3]$$

$$= \frac{e^{i\omega t}}{4\pi^2 R D_e} \{K_0(\kappa r_0) I_0(\kappa r) - K_0(\kappa a) I_0(\kappa r_0) I_0(\kappa r)/I_0(\kappa a)\} \qquad r < r_0$$

$$= \frac{e^{i\omega t}}{4\pi^2 R D_e} \{K_0(\kappa r) I_0(\kappa r_0) - K_0(\kappa a) I_0(\kappa r_0) I_0(\kappa r)/I_0(\kappa a)\} \qquad r > r_0$$

where $\kappa \equiv (i\omega/D_e)^{1/2}$ and I and K are modified Bessel functions of a complex argument. For an arbitrarily distributed source $s(r, \omega$ the solution is obtained by integrating the Green's function:

$$\tilde{n}_e(r,t) = \int s(r_0, \omega)\, \tilde{n}_e^{\delta}(r, t, r_0, \omega, D_e)\, dr_0 d\omega \qquad [4]$$

The electron source is assumed to be of the form: $\tilde{S}_e = S_a \cdot e^{(r-a)/\lambda}$. Thus there are 3 free parameters: D_e, S_a, and λ. The physics of the problem is governed by the dimensionless parameter $\gamma = \lambda(\omega/D_e)^{1/2}$. For $\gamma \ll 1$ the localisation of the source can not be resolved.

Note that the linearized electron source distribution is not necessarily identical with the 0-th order distribution if impurity ionisation contributes significantly to

the source. Because non-hydrogenic species can not penetrate the discharge by multiple charge exchange, the contribution of light impurities to the particle source is shallower than that of the hydrogenic species and λ is an upper bound for the penetration of the 0-th order electron source.

3. MEASUREMENTS OF THE ELECTRON SOURCE DISTRIBUTION

Figure 1 shows the evolution of a 3 MA, 3.1 T, X-point discharge with 1 Hz modulation of the gas feed. 7 channels of the reflectometer have critical densities in the plasma. A least-squares fit to the data yields $\lambda < a/40$, where a is the equivalent minor radius. Figure 2 shows the sensitivity of the simulations to λ The results are not sensitive to values of $\lambda \leq a/20$ (because γ becomes too small) and this should be considered as an upper bound on the source decay length. Comparison with the density modulations infered from Abel inversion of the interferometer data show that this diagnostic does not have sufficient spatial resolution to resolve the particle source distribution. The modulation amplitudes decrease rapidly with modulation frequency and the signals become noisy. Nevertheless, similar results are obtained for modulation at 4 Hz: $\lambda = a/20$. See figure 3.

In a steady-state impurity-free plasma, the electron source can be calculated from the rates of electron ionization and recombination:

$$S_e = n_e(n_n^E + n_n^R) < \sigma v >_I - n_e n_i < \sigma v >_R \qquad [5]$$

where n_e and n_i are the densities of electrons and ions, n_n^E is the neutral density transported from the edge by multiple charge-exchange, and n_n^R is the neutral density arising from recombination. The subscripts I and R refer to ionization and recombination processes. For the discharges considered here recombination is relatively unimportant and is neglected.

Figure 4 compares the electron source distribution calculated in this manner by the 3-D neutral transport code AURORA3 with that determined by gas modulation. The modulation results confirm the shallow penetration of the electron source in JET. Note that the calculated source does not have a simple exponential form. It has a tail which reflects the deep penetration of neutrals through multiple charge exchange but which is not of sufficiently large amplitude to contribute significantly to the particle balance.

For the purpose of calculating the electron flux, the total electron source is determined by normalising the source profile to D_α measurements of the deuterium ionization at the limiters and vessel walls. The contribution from impurities is estimated assuming a continuous transition from Be (Z=4) being the dominant impurity at low-Z_{eff} to C (Z=6) being the dominant impurity at high-Z_{eff}.

4. ELECTRON FLUX ANALYSIS

Once the electron source is known, the electron flux can be calculated from the continuity equation:

$$\frac{\partial n_e(r,t)}{\partial t} = -\nabla \bullet \Gamma_e(r,t) + S_e(r,t) \qquad [6]$$

The forces driving the electron flux are not known. Various possibilities have been discussed in the literature /14,15,16/. We adopt a conventional model /17,18/ and express the electron flux as the sum of a diffusive flux and an unspecified "convective" flux which incorporates any additional terms not dependent on the density gradient:

$$\Gamma_e = -D_e \nabla n_e + n_e V_p \qquad [7]$$

With constant transport coefficients, equation 7 implies that a graph of the radial electron velocity Γ_e/n_e versus the inverse density scale length $-\nabla n_e/n_e$ during a density transient produces a straight line whose slope is D_e and whose y-intercept is V_p. An analogous method has been applied to thermal transport analysis /19/. This linear relation is shown in figure 5 for the gas-modulation experiment discussed in the previous section, validating the ansatz for the form of the electron flux.

The calculated diffusion coefficient and pinch velocity are shown in figures 6 and 7. We note that the value of the diffusion coefficient at large radii is in good agreement with the analysis of the reflectometer signal modulations described in section 2, which yields $D_e = 0.75 m^2\,\mathrm{sec}^{-1}$ for the same discharge. Both the diffusion coefficient and the pinch velocity increase with radius. In the outer portion of the plasma the particle pinch velocity exceeds the neo-classical value by nearly an order of magnitude. These characteristics were previously inferred from the modelling of ICRF-induced density transients /4/.

Since the transients studied here are accompanied by high power heating and large density excursions, this technique cannot be considered non-perturbative. However, a comparison with coefficients obtained from non-perturbing techniques such as sawtooth pulse propagation and injection of small pellets shows good agreement with those from this method /3/.

The statistical error in the determination of D_e is 10 %. The absolute error in D_e arises principally from errors in the density gradient and the electron source. The error in the density gradient is estimated by considering the propagation of errors in the Abel-inversion procedure (using the covariance matrix of the expansion coefficients of the line-integrated density data). It gives rise to an error of 40% in D_e for $0.4 < r/a < 0.8$. The error in the electron source is estimated assuming an error of a factor of 2 in the source scale length. At $r/a = 0.7$ this leads to a 10% error in D_e. These errors are partly systematic and can not be added in quadrature. Thus the error in D_e is approximately 50% at $r/a = 0.7$. The error tends to increase both at small radii, due to decreasing variation in the inverse density scale length, and at large radii, due to increasing sensitivity to the electron source distribution.

The most important source of error is the uncertainty in the electron density gradient. However there is good agreement among the reflectometer, interferometer and LIDAR (Thomson scattering) density profiles in this discharge. See figure 8. (Note that the reflectometer profile is formally

double-valued at $R \sim 4m.$, owing to the nature of this measurement which gives the position of given density layers rather than the density at given positions.)

5. SCALING OF TRANSPORT COEFFICIENTS

In order to determine the scaling of the particle transport coefficients, the flux analysis described in the previous section was extended to a number of JET discharges covering the parameter range: $1.5 < I_p < 6\,MA$, $0 < P_{add} < 16\,MW$, $7 \cdot 10^{18} < \langle n_e \rangle < 4.2 \cdot 10^{19} m^{-3}$, $1.3 < Z_{eff} < 3.8$. The data are in a narrow range of toroidal field ($2.9 < B_T < 3.2\,T$) so that any dependence on this parameter can not be examined.

The analysis was restricted to transients having an excursion of at least 15% in the parameter $\nabla n_e/n_e$ and yielding transport coefficients with a statistical error of less than 30%.

A non-linear regression, using local plasma parameters, of the form

$$D_e(r/a = 0.7) = C B_p^{\alpha_B} T_e^{\alpha_T} n_e^{\alpha_n} Z_{eff}^{\alpha_Z} \qquad [8]$$

yields $\alpha_B = -0.3$, $\alpha_T = 1.1$, and C = 0.24 when D_e is expressed in $m_2/sec.$, B_p in Tesla and T_e in KeV. No marked dependence on density or effective charge is found. Although this regression fits the data within their error bars (see figure 9), the errors in the exponents are of the order of the exponents themselves. This is due to a colinearity in the data set which can be expressed as $B_p \sim T_e^{0.6}$, and which subsits even though the data were specifically chosen to maximise the variation of electron temperature at a given plasma current. For example, dividing eq. 8 by $\sim \sqrt{B_p/T_e^{0.6}}$ only increases the RMS error by 15%. In summary, the diffusion coefficient increases with electron temperature and decreases with poloidal magnetic field, but the data are not of sufficient quality to determine these dependences exactly. Similar dependences have been put forward for thermal transport /20/.

The pinch velocity is found to be proportional to the diffusion coefficient, suggesting that a common mechanism gives rise to both transport coefficients. See figure 10.

6. CONCLUSIONS

The good spatial resolution of the reflectometer measurements allows the electron source distribution to be determined. The results confirm the shallow penetration predicted by neutral transport codes. Electron particle transport in JET is well described by a model of the flux which consists of diffusive and convective components. The diffusion coefficient is one or two orders of magnitude larger than the neo-classical value. It has a hollow radial profile and scales with the electron temperature and inversely with the poloidal magnetic field. The particle pinch velocity exceeds the neo-classical value by an order of magnitude at radii larger than $r/a \sim 0.4$, and has a scaling similar to that of the diffusion coefficient.

REFERENCES

/1/ J A Wesson et al, Nuclear Fusion 29(1989)641

/2/ B Lipschultz, B LaBombard, E S Marmar et al, Nuclear Fusion 24(1984)997.

/3/ A Gondhalekar, A D Cheetham, J C M de Haas et al, Plasma Physics and Controlled Fusion 31(1989)805.

/4/ A Gondhalekar et al, Bull. Am. Phys. Soc. 30(1985)1525
and JET Report JET-P(85)31

/5/ M H Hughes and D E Post, PPPL Report 1335

/6/ S Corti, G Bracco, M Brusati et al, Controlled Fusion and Plasma Heating (12th Euro. Conf., Budapest, 1985), European Physical Society, 1985, Part I, p 219.

/7/ P D Morgan et al, Review of Scientific Instruments 56(1985)862.

/8/ P D Morgan and J O'Rourke, Controlled Fusion and Plasma Heating (14th Euro. Conf., Madrid, 1987), European Physical Society, 1987, Part III, p 1240.

/9/ R Prentice, P Cripwell, A E Costley, et al, Controlled Fusion and Plasma Heating (15th Euro. Conf., Dubrovnik, 1988), European Physical Society, 1988, Part III, p 1115.

/10/ G Braithwaite, G Magyar, J O'Rourke et al, Review of Scientific Instruments 60(1989)2825.

/11/ H Salzmann, J Bundgaard, A Gadd et al, Review of Scientific Instruments 59(1988)1451.

/12/ B J D Tubbing, E Barbian, D J Campbell, et al, Controlled Fusion and Plasma Physics (12th Euro. Conf., Budapest, 1985), European Physical Society, 1985, Part I, p 215.

/13/ E Barbato and R Giannella, Physics Letters 110A (1985)309

/14/ F L Hinton R D Hazeltine, Review of Modern Physics, 48(1976)239.

/15/ R Capes C Mercier, Plasma Physics and Controlled Nuclear Fusion Research, 1982 (Proc. 9th Int. Conf., Baltimore, 1982), IAEA, Vienna, (1983), Vol. I, p.337.

/16/ J O'Rourke, Nuclear Fusion 27(1987)2075.

/17/ B Coppi and N Sharky, Nuclear Fusion 21(1981)1365.

/18/ K Behringer et al, Bull. Am. Phys. Soc. 25(1980)875

/19/ J D Callen, J P Christiansen, J G Cordey et al, Nuclear Fusion 27(1987)1857.

/20/ J P Christiansen, J G Cordey, K Thomsen, et al, Nuclear Fusion 31(1991)2117.

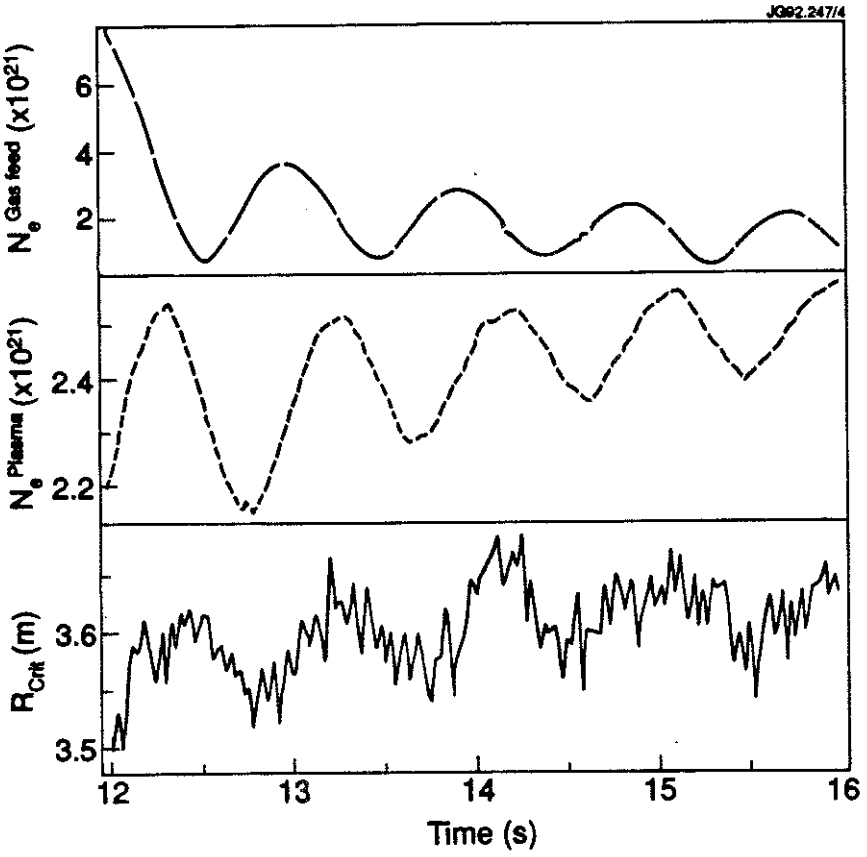

Fig. 1 -- Evolution of the gas feed, particle inventory and major radius of $n_e^{crit} = 2.5 \cdot 10^{19} m^{-3}$ in pulse 24248 (1. Hz modulation).

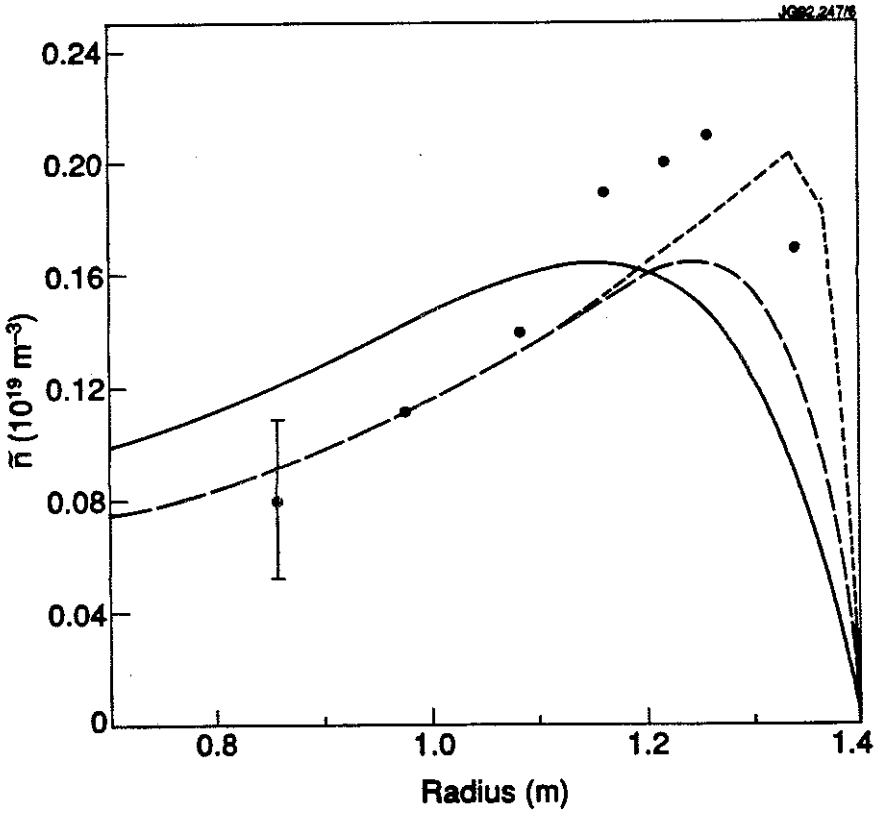

Fig. 2 -- Modulation amplitude versus minor radius in pulse 24248. Reflectometer data (circles), $\lambda = a/5$ (solid line), $\lambda = a/20$ (dotted line), $\lambda = a/80$ (dashed line).

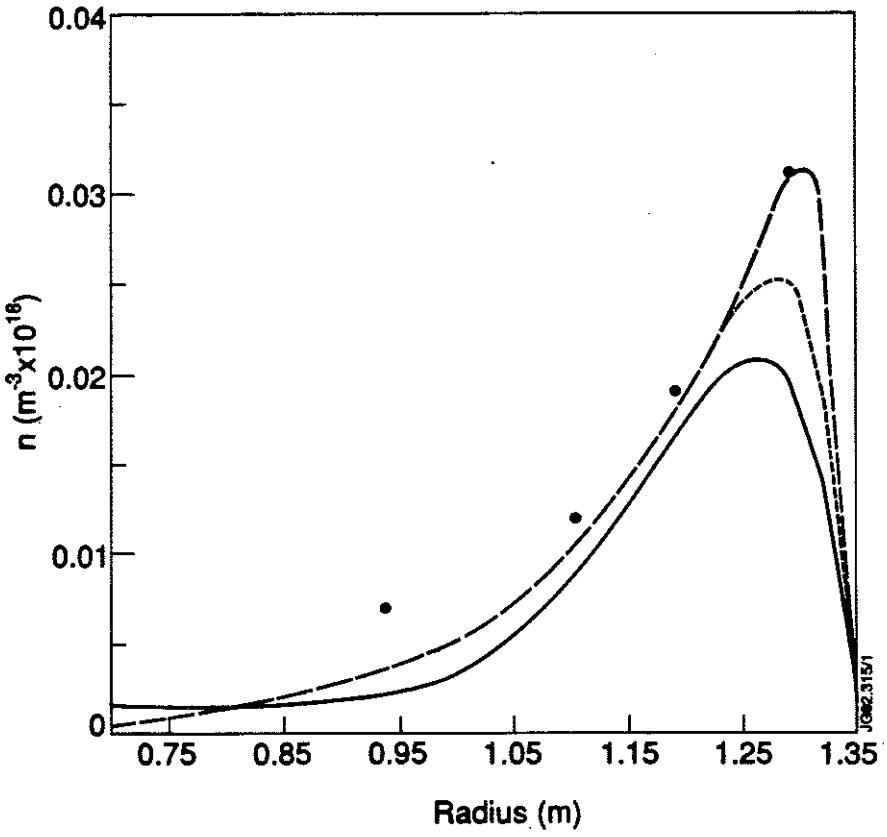

Fig. 3 -- Modulation amplitude versus minor radius in pulse 27204. Reflectometer data (circles), $\lambda = a/5$ (solid line), $\lambda = a/20$ (dotted line), $\lambda = a/80$ (dashed line).

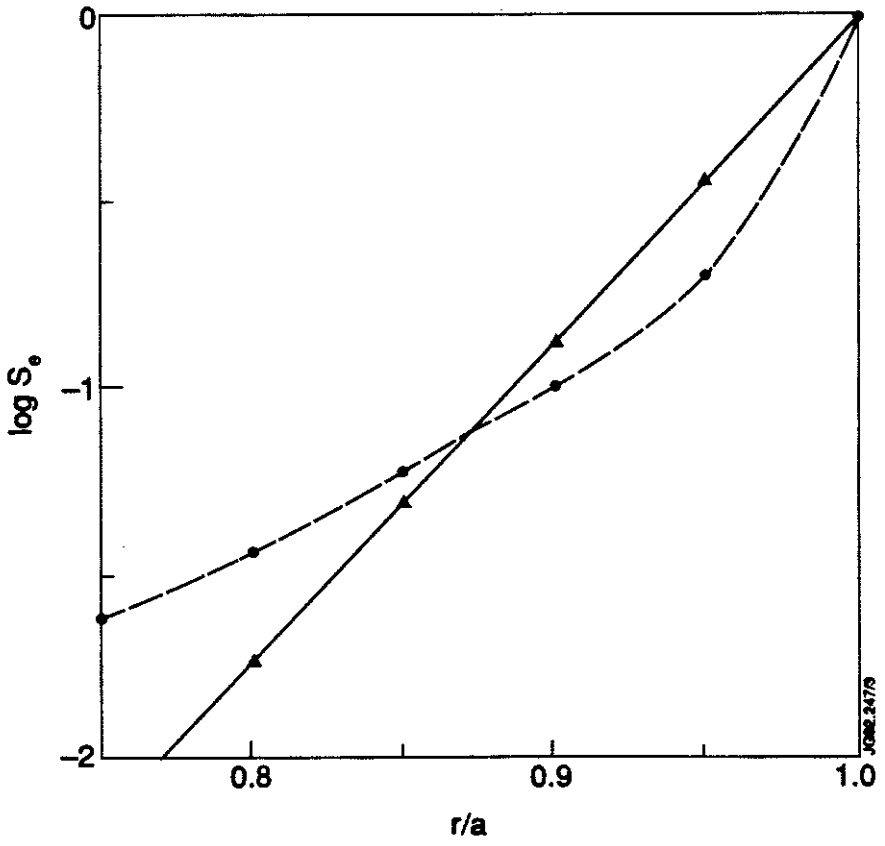

Fig. 4 -- Calculated (circles) and experimentally determined (triangles) electron source distribution versus r/a in pulse 24248.

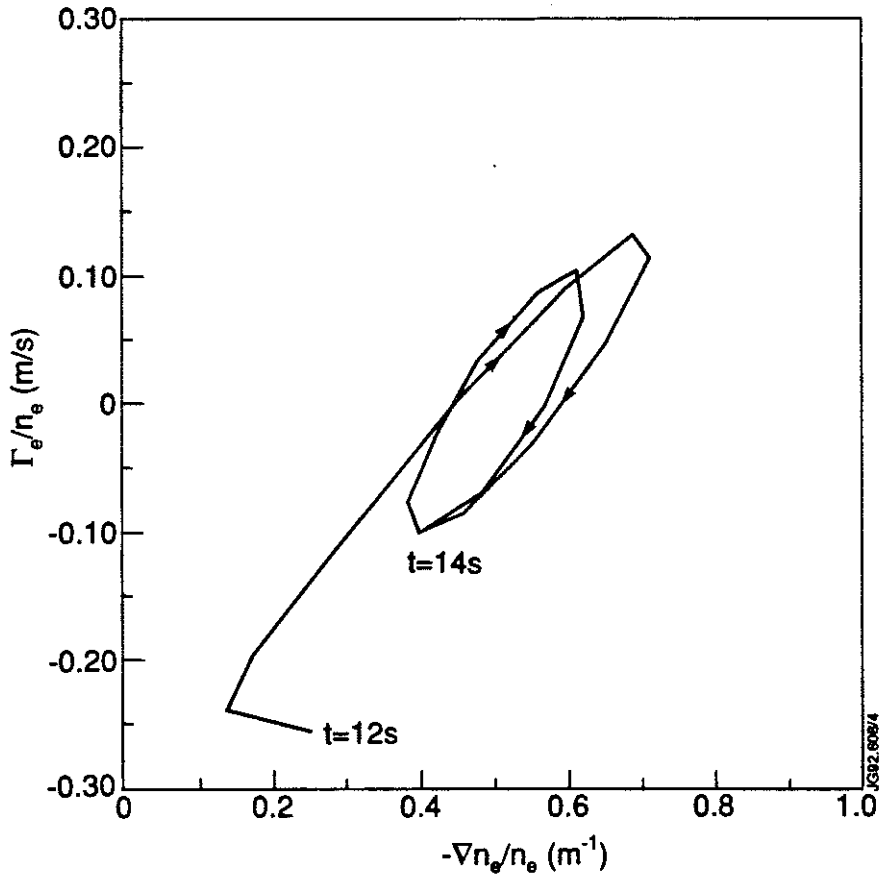

Fig. 5 -- Electron flux (calculated using the experimentally determined source) versus density gradient at r/a = 0.7 in pulse 24248.

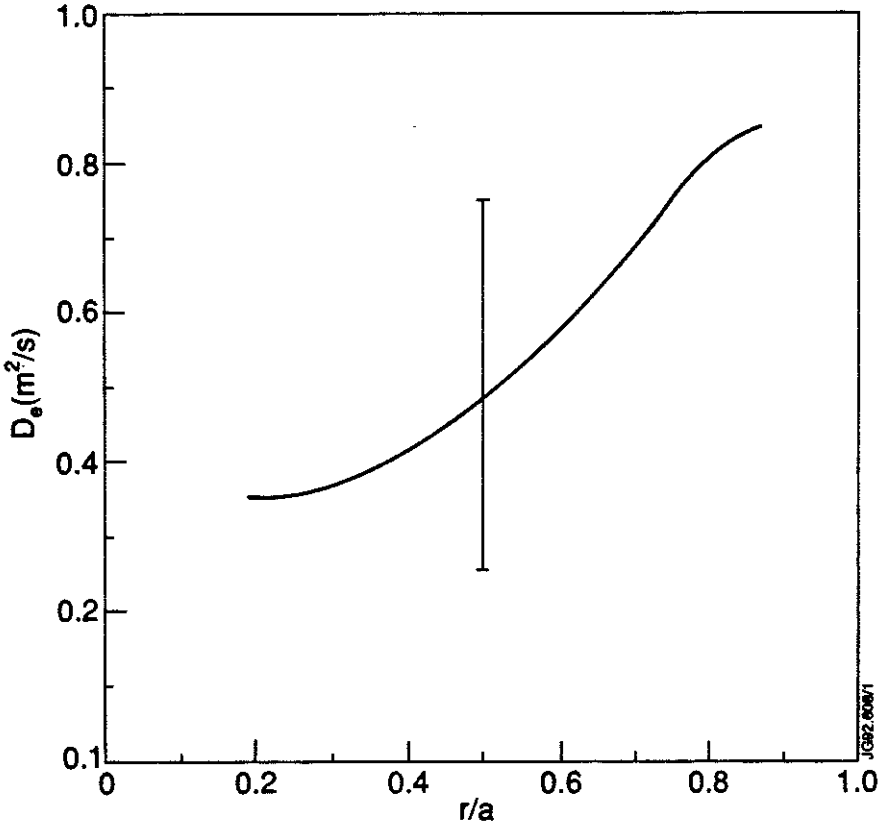

Fig. 6 -- Diffusion coefficient versus r/a from time-dependent flux analysis.

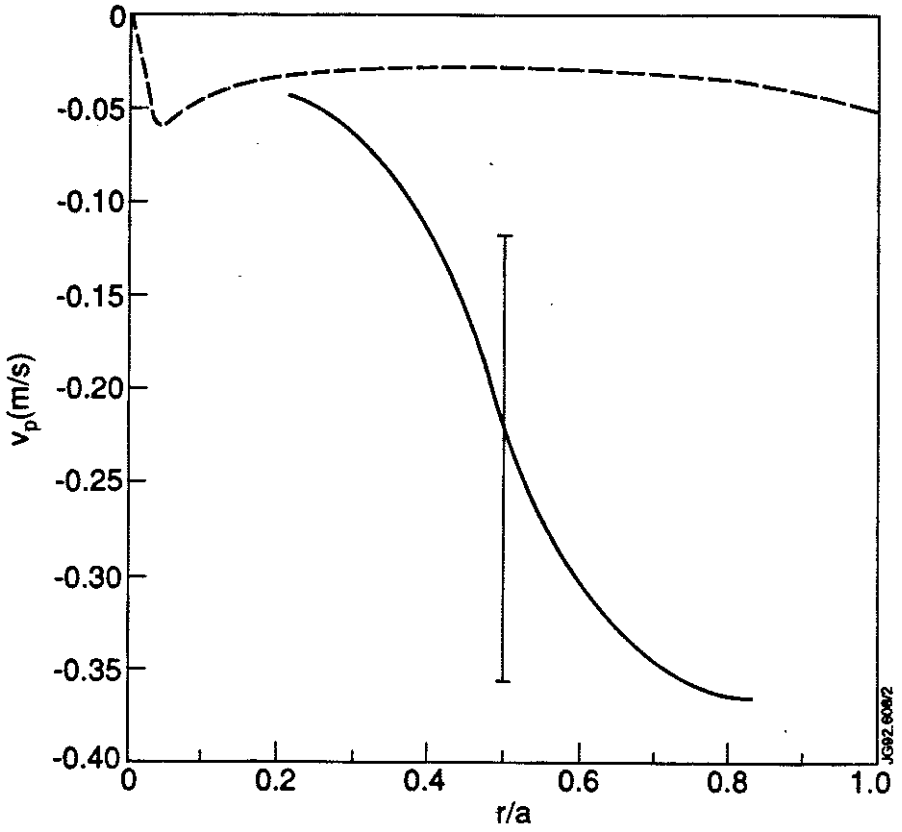

Fig. 7 -- Pinch velocity versus r/a from time-dependent flux analysis. Also shown is the neo-classical pinch velocity (dashed line).

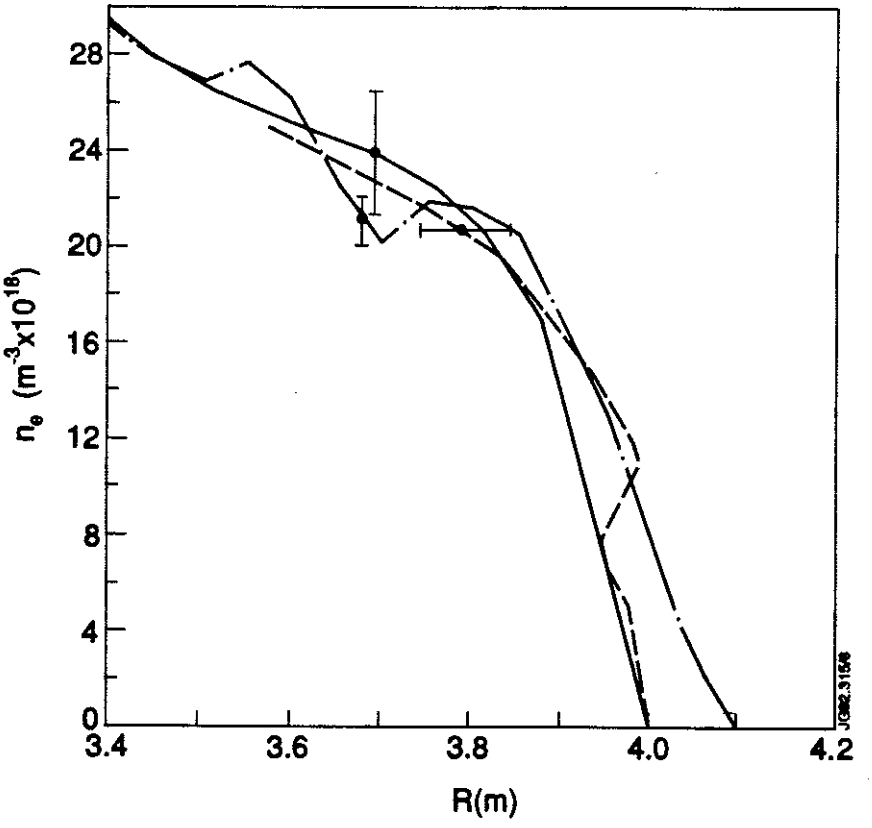

Fig. 8 -- Electron density profiles in pulse 24248. Interferometric data (solid line), reflectometer data (dotted line), Thomson scattering (LIDAR) data (--- • ---).

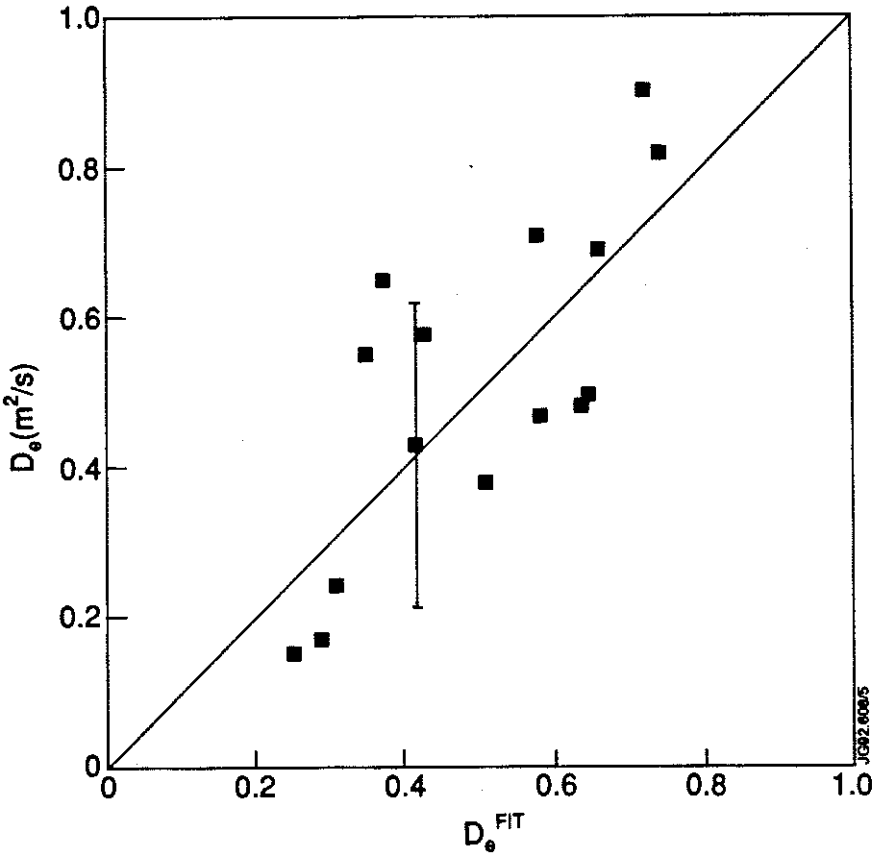

Fig. 9 -- Diffusion coefficient versus fit at r/a = 0.7.

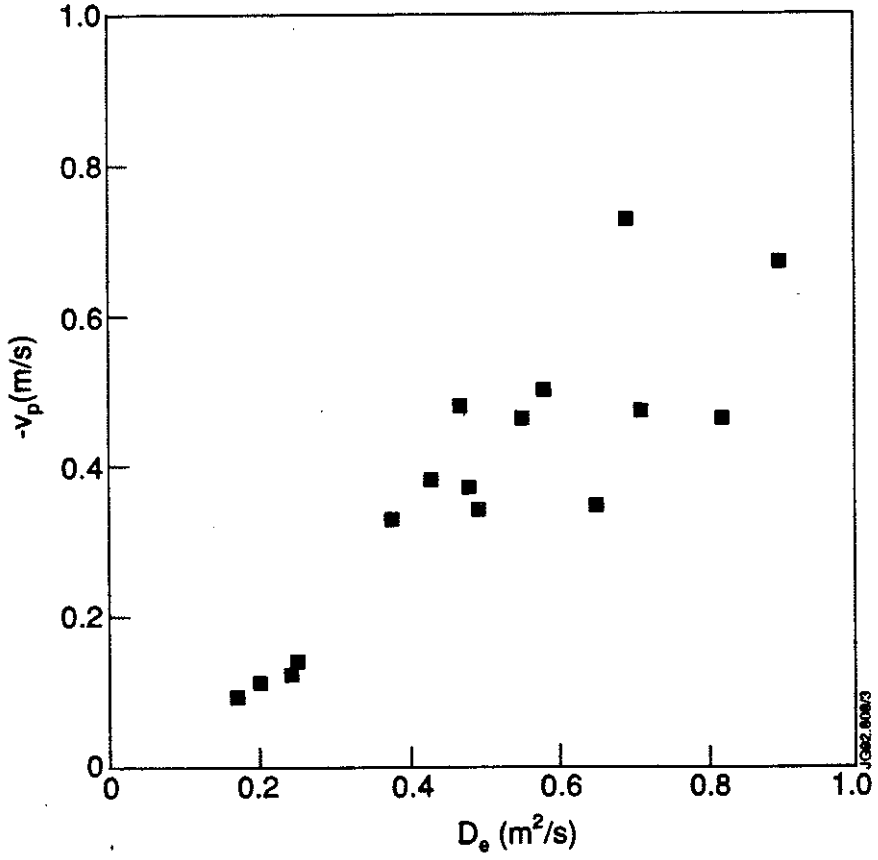

Fig. 10 -- Pinch velocity versus Diffusion coefficient at r/a = 0.7.

Appendix I

THE JET TEAM

JET Joint Undertaking, Abingdon, Oxon, OX14 3EA, U.K.

J.M. Adams[1], B. Alper, H. Altmann, A. Andersen[14], P. Andrew, S.Ali-Arshad, W. Bailey, B. Balet, P. Barabaschi, Y. Baranov, P. Barker, R. Barnsley[2], M. Baronian, D.V. Bartlett, A.C. Bell, G. Benali, P. Bertoldi, E. Bertolini, V. Bhatnagar, A.J. Bickley, D. Bond, T. Bonicelli, S.J. Booth, G. Bosia, M. Botman, D. Boucher, P. Boucquey, M. Brandon, P. Breger, H. Brelen, W.J. Brewerton, H. Brinkschulte, T. Brown, M. Brusati, T. Budd, M. Bures, P. Burton, T. Businaro, P. Butcher, H. Buttgereit, C. Caldwell-Nichols, D.J. Campbell, D. Campling, P. Card, G. Celentano, C.D. Challis, A.V.Chankin[23], A. Cherubini, D. Chiron, J. Christiansen, P. Chuilon, R. Claesen, S. Clement, E. Clipsham, J.P. Coad, I.H. Coffey[24], A. Colton, M. Comiskey[4], S. Conroy, M. Cooke, S. Cooper, J.G. Cordey, W. Core, G. Corrigan, S. Corti, A.E. Costley, G. Cottrell, M. Cox[7], P. Crawley, O. Da Costa, N. Davies, S.J. Davies[7], H. de Blank, H. de Esch, L. de Kock, E. Deksnis, N. Deliyanakus, G.B. Denne-Hinnov, G. Deschamps, W.J. Dickson[19], K.J. Dietz, A. Dines, S.L. Dmitrenko, M. Dmitrieva[25], J. Dobbing, N. Dolgetta, S.E. Dorling, P.G. Doyle, D.F. Düchs, H. Duquenoy, A. Edwards, J. Ehrenberg, A. Ekedahl, T. Elevant[11], S.K. Erents[7], L.G. Eriksson, H. Fajemirokun[12], H. Falter, J. Freiling[15], C. Froger, P. Froissard, K. Fullard, M. Gadeberg, A. Galetsas, L. Galbiati, D. Gambier, M. Garribba, P. Gaze, R. Giannella, A. Gibson, R.D. Gill, A. Girard, A. Gondhalekar, D. Goodall[7], C. Gormezano, N.A. Gottardi, C. Gowers, B.J. Green, R. Haange, A. Haigh, C.J. Hancock, P.J. Harbour, N.C. Hawkes[7], N.P. Hawkes[1], P. Haynes[7], J.L. Hemmerich, T. Hender[7], J. Hoekzema, L. Horton, J. How, P.J. Howarth[5], M. Huart, T.P. Hughes[4], M. Huguet, F. Hurd, K. Ida[18], B. Ingram, M. Irving, J. Jacquinot, H. Jaeckel, J.F. Jaeger, G. Janeschitz, Z. Jankowicz[22], O.N. Jarvis, F. Jensen, E.M. Jones, L.P.D.F. Jones, T.T.C. Jones, J-F. Junger, F. Junique, A. Kaye, B.E. Keen, M. Keilhacker, W. Kerner, N.J. Kidd, R. Konig, A. Konstantellos, P. Kupschus, R. Lässer, J.R. Last, B. Laundy, L. Lauro-Taroni, K. Lawson[7], M. Lennholm, J.Lingertat[13], R.N. Litunovski, A. Loarte, R. Lobel, P. Lomas, M. Loughlin, C. Lowry, A.C. Maas[15], B. Macklin, C.F. Maggi[16], G. Magyar, V. Marchese, F. Marcus, J. Mart, D. Martin, E. Martin, R. Martin-Solis[8], P. Massmann, G. Matthews, H. McBryan, G. McCracken[7], P. Meriguet, P. Miele, S.F. Mills, P. Millward, E. Minardi[16], R. Mohanti[17], P.L. Mondino, A. Montvai[3], P. Morgan, H. Morsi, G. Murphy, F. Nave[27], S. Neudatchin[23], G. Newbert, M. Newman, P. Nielsen, P. Noll, W. Obert, D. O'Brien, J. O'Rourke, R. Ostrom, M. Ottaviani, S. Papastergiou, D. Pasini, B. Patel, A. Peacock, N. Peacock[7], R.J.M. Pearce, D. Pearson[12], J.F. Peng[26], R. Pepe de Silva, G. Perinic, C. Perry, M.A. Pick, J. Plancoulaine, J-P. Poffé, R. Pohlchen, F. Porcelli, L. Porte[19], R. Prentice, S. Puppin, S. Putvinskii[23], G. Radford[9], T. Raimondi, M.C. Ramos de Andrade, M. Rapisarda[29], P-H. Rebut, R. Reichle, S. Richards, E. Righi, F. Rimini, A. Rolfe, R.T. Ross, L. Rossi, R. Russ, H.C. Sack, G. Sadler, G. Saibene, J.L. Salanave, G. Sanazzaro, A. Santagiustina, R. Sartori, C. Sborchia, P. Schild, M. Schmid, G. Schmidt[6], H. Schroepf, B. Schunke, S.M. Scott, A. Sibley, R. Simonini, A.C.C. Sips, P. Smeulders, R. Smith, M. Stamp, P. Stangeby[20], D.F. Start, C.A. Steed, D. Stork, P.E. Stott, P. Stubberfield, D. Summers, H. Summers[19], L. Svensson, J.A. Tagle[21], A. Tanga, A. Taroni, C. Terella, A. Tesini, P.R. Thomas, E. Thompson, K. Thomsen, P. Trevalion, B. Tubbing, F. Tibone, H. van der Beken, G. Vlases, M. von Hellermann, T. Wade, C. Walker, D. Ward, M.L. Watkins, M.J. Watson, S. Weber[10], J. Wesson, T.J. Wijnands, J. Wilks, D. Wilson, T. Winkel, R. Wolf, D. Wong, C. Woodward, M. Wykes, I.D. Young, L. Zannelli, A. Zolfaghari[28], G. Zullo, W. Zwingmann.

PERMANENT ADDRESSES

1. UKAEA, Harwell, Didcot, Oxon, UK.
2. University of Leicester, Leicester, UK.
3. Central Research Institute for Physics, Budapest, Hungary.
4. University of Essex, Colchester, UK.
5. University of Birmingham, Birmingham, UK.
6. Princeton Plasma Physics Laboratory, New Jersey, USA.
7. UKAEA Culham Laboratory, Abingdon, Oxon, UK.
8. Universidad Complutense de Madrid, Spain.
9. Institute of Mathematics, University of Oxford, UK.
10. Freien Universität, Berlin, F.R.G.
11. Royal Institute of Technology, Stockholm, Sweden.
12. Imperial College, University of London, UK.
13. Max Planck Institut für Plasmaphysik, Garching, FRG.
14. Risø National Laboratory, Denmark.
15. FOM Instituut voor Plasmafysica, Nieuwegein, The Netherlands.
16. Dipartimento di Fisica, University of Milan, Milano, Italy.
17. North Carolina State University, Raleigh, NC, USA
18. National Institute for Fusion Science, Nagoya, Japan.
19. University of Strathclyde, 107 Rottenrow, Glasgow, UK.
20. Institute for Aerospace Studies, University of Toronto, Ontario, Canada.
21. CIEMAT, Madrid, Spain.
22. Institute for Nuclear Studies, Otwock-Swierk, Poland.
23. Kurchatov Institute of Atomic Energy, Moscow, USSR
24. Queens University, Belfast, UK.
25. Keldysh Institute of Applied Mathematics, Moscow, USSR.
26. Institute of Plasma Physics, Academica Sinica, Hefei, P. R. China.
27. LNETI, Savacem, Portugal.
28. Plasma Fusion Center, M.I.T., Boston, USA.
29. ENEA, Frascati, Italy.

At 1st July, 1992